*IFSCC 2025 full paper (IFSCC2025-829)*

# *"A Novel Green Technology of Multifunctional Nanozyme and Its Potential Application in Skin Care"*

**Xiaojuan Yan [1,2]*, Manhong Liu [2] and Jiaqi Miao [2]**

[1] Shanghai Meicui Biological Science and Technology Ltd. Co., Shanghai, China;
[2] Meicui Beauty and Health Science and Innovation Center, Shanghai, China

## 1. Introduction

Nanozymes (NMs), also known as catalytic antioxidants, have emerged as promising alternatives to natural enzymes due to their high stability and versatility properties [1, 2]. NMs have been reported to be synthesized by combining natural polyphenols (e.g. tannic acid, epigallocatechin gallate) with metal ions (e.g. $Cu^{2+}$, $Zn^{2+}$) in an easy, green and sustainable way [3]. These designed NMs, composed of biocompatible and biodegradable materials, could exhibit reduced toxicity and versatile activities. NMs have been demonstrated to possess numerous advantages, including low cost, tunable catalytic activity, and exceptional stability, which has attracted much attention and research progress in cancer therapeutics, oral ulcers, skin wound repair, and biosensing [4-8].

According to the previous studies, conventional methods for NMs preparation, including hydrothermal method, solvothermal method, co-precipitation method, sol-gel method, and other methods [9]. There are critical limitations of agglomeration induced deactivation due to the inhomogeneous distribution of catalytic active sites, and potential biocompatibility risks from residual toxic solvents (e.g., organic amines, methanol) [10].

In this study, a novel multifunctional nanozyme technology has been proposed for skin care or therapeutics. Based on the metal ion-polyphenol interaction mechanism, a series of versatile NMs were developed. The efficacy of the NMs was further evaluated by various *in vitro* assays. The microstructure of the NMs was studied using various analytical techniques, including Fourier transform infrared spectra (FTIR), ultraviolet absorption spectrometer (UV-vis) and X-ray photoelectron spectroscopy (XPS). The interaction between molecules to form NMs was demonstrated and these NMs were shown to have unique antioxidant and antimicrobial activities. Furthermore, these versatile NMs were formulated into a range of skin care products, including shampoo, lotion, gel and cream. The NMs-containing formulation showed good safety, stability and efficacy, suggesting its potential as a promising solution for skin treatment.

## 2. Materials and Methods

2.1 Chemicals and reagents

(-)-Epigallocatechin gallate (EGCG, purity>98%), Zinc gluconate (CGZn, purity>98%), Copper gluconate (CGCu, purity>98%), $Ti(SO_4)_2$ (purity>98%), 2,2-diphenyl-1-picrylhydrazyl (DPPH, purity>98%) and $H_2O_2$ (purity>98%) were purchased from D&B Biological and Macklin Co. Ltd. *Malassezia furfur* (*M. furfur,* lot: BNCC358921) and *Cutibacterium acnes* (*C. acnes*, Lot: BNCC336649) were purchased from BeNa Culture Collection Co. Ltd.

2.2 Preparation of EGCG NMs

EGCG NMs were prepared by an oxidative coupling assembly strategy. EGCG-Cu NMs were prepared by the coordination of EGCG and metal ions. First, poly(vinyl alcohol) (PVP, $M_W$: 1000) and sodium dodecyl sulfate (SDS, 99% purity) were dissolved independently in deionized water. The EGCG and CGCu or CGZn solutions were then added individually to the solution at a ratio of 1:10 (w/w) and the solution was thoroughly mixed. After adjusting the pH to 5.5-7.5 with NaOH (2 M), the solution was heated to 50°C and incubated for a period of 3 hours. The EGCG NMs solution was then prepared. The freeze-dried powder of EGCG NMs could also be obtained by lypophilization under vacuum overnight.

2.3 Characterization of EGCG NMs

The microstructure of EGCG NMs was characterized by Fourier transform infrared spectroscopy (FTIR, VERTEX 70, Bruck, Germany) and UV-vis absorption spectroscopy (UV-vis, V-770, JASCO, Japan). X-ray photoelectron spectroscopy (XPS) of NMs was performed using with an X-ray monochromator (XR5 Gun-500 μm, Thermo scientific, USA).

2.4 Antioxidant activity assay

The antioxidant activity of EGCG NMs was evaluated by various *in vitro* assays, including DPPH, OH radical (·OH) and $H_2O_2$ scavenging assays [11-14]. These EGCG NMs were prepared at concentrations of 0.05~20 mg/mL. 100 μL of the solution was added to 100 μL of ethanol solution containing 200 μmol/L DPPH. L-ascorbic acid and deionized water were used as positive and control groups, respectively. After shaking, the plates were kept in the dark at room temperature for 30 minutes. The absorbance of the different groups was determined at 517 nm.

The ·OH scavenging activity of EGCG NMs was further evaluated by a method based on the Fenton reaction, which is widely used for antioxidant screening [15]. The initiation of the ·OH reaction was generated by adding $0.2\times10^{-3}$ mol/L $H_2O_2$ and $0.2\times10^{-3}$ mol/L $FeSO_4$ and mixing for 3 minutes. EGCG NMs were then added to the solution and incubated for a further 3 minutes. Finally, $1.0\times10^{-3}$ mol/L salicylic acid (SA) was added to detect the remaining OH radicals. SA was oxidized by OH radicals to 2,3-dihydroxybenzoic acid with an absorbance peak at 510 nm. The remaining OH radicals were quantified by UV absorption and the scavenging percentage of OH radicals was calculated.

The $H_2O_2$ scavenging activity of EGCG NMs was determined by the $Ti(SO_4)_2$ assay. To prepare $H_2O_2$ indicator, 25 mg of $Ti(SO_4)_2$ was dissolved in $H_2SO_4$ solution (3 M, 25 mL). 200 μL of indicator was added to 100 μL of $H_2O_2$ solutions of different concentrations (0.2, 0.4, 0.6, 1, 2, 4 mM) to measure the absorbance at 407 nm for the standard curve of hydrogen peroxide. Samples of different concentrations were mixed evenly with 4 mL of $H_2O_2$ (1 mM) and incubated at 37 °C. After incubation for 2 hours, 100 μL of the mixed solution was added to 200 μL of the

indicator. The absorbance of the solution at 407 nm was detected using an enzyme-linked immunosorbent assay reader. The $H_2O_2$ scavenging efficiency of the NMs was calculated.

Methodology for Minimum Bactericidal Concentration (MBC) Assay

The antibacterial activity of the EGCG NMs was evaluated by determining the minimum bactericidal concentration (MBC) against *C. acnes* and *M. furfur.* The *C. acnes* and *M. furfur* were incubated at a concentration of $10^6$ CFU/mL with different concentrations of EGCG NMs (0.1~10 mg/mL) for 24 hours in their respective broths. The untreated group was used as a negative control. 100 µL aliquots were plated on Luria-Bertani (LB) agar and incubated at 37 °C for 24 hours. MBC was determined by the lowest concentration that achieved ≥ 99.9% reduction in viable CFU compared to the control.

## 3. Results

3.1 Synthesis and characterization of EGCG NMs

EGCG-Zn and EGCG-Cu NMs were synthesized by an easy and green method using oxidative coupling assembly of EGCG with $Cu^{2+}$ and $Zn^{2+}$, respectively. The processes were carried out and screened by precursor concentrations under different pH values.

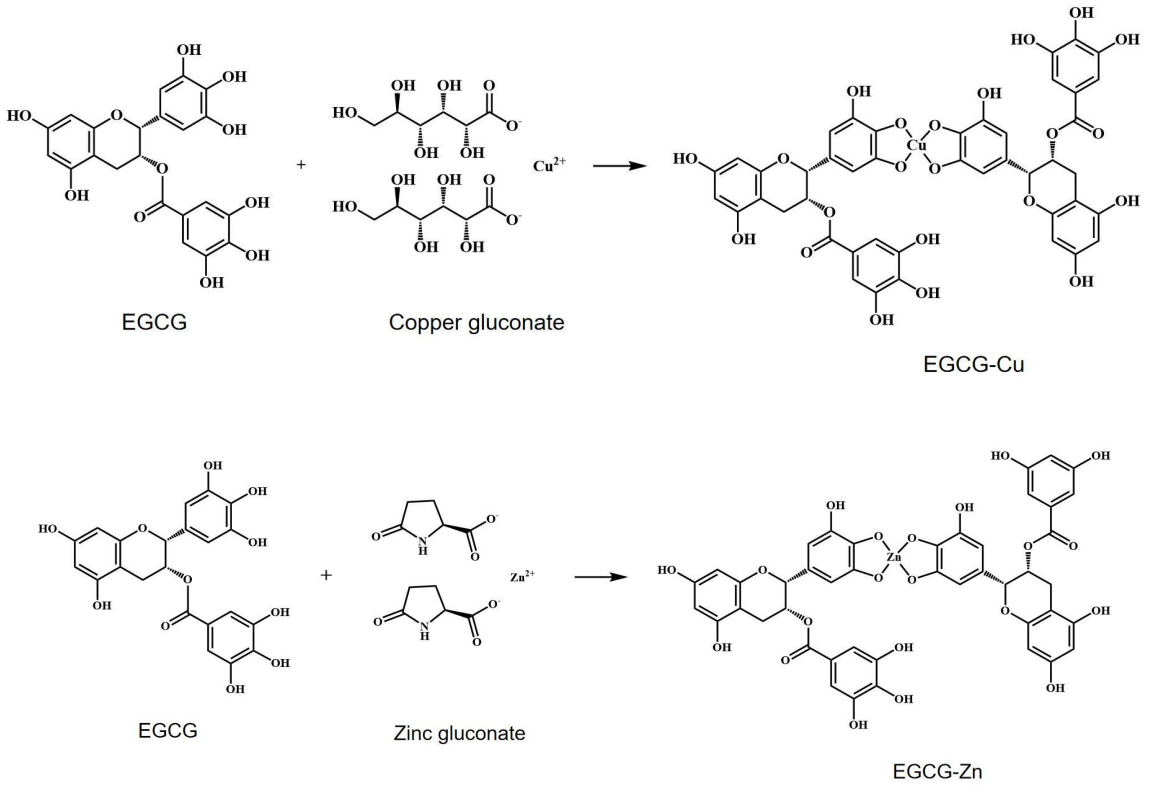


**Figure 1.** Synthesis process of EGCG-Cu and EGCG-Zn NMs.

3.2 Characterization of EGCG NMs

The EGCG-Zn and EGCG-Cu NMs were obtained and their microstructures were confirmed by UV-vis, FTIR and XPS analysis. As shown in Figure 2a, the UV-vis spectra of EGCG, EGCG-Zn and EGCG-Cu NMs were scanned. The characteristic wavelength of EGCG, which

was found to be 274 nm, was shifted to 315 nm and 324 nm for the characteristic absorption wavelengths of EGCG-Cu and EGCG-Zn NMs, respectively.

The characteristic FTIR absorption spectra of EGCG, EGCG-Zn and EGCG-Cu NMs were further examined. As shown in Figure 2b, the characteristic absorption peak centered at 3357 $cm^{-1}$ of EGCG was obviously shifted to 3431 $cm^{-1}$ and 3416 $cm^{-1}$ for EGCG-Cu and EGCG-Zn, respectively. The peak at 1692 $cm^{-1}$ and the fingerprint regions around 1086 $cm^{-1}$ and 627 $cm^{-1}$ of the FTIR spectra between EGCG and EGCG NMs were different from each other.

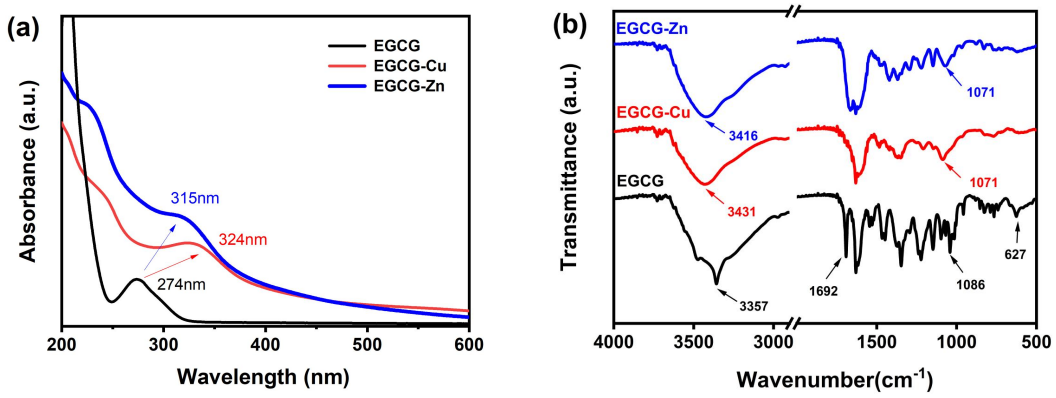


**Figure 2.** (a) UV–vis and (b) FTIR absorption spectra of EGCG, EGCG-Cu NMs and EGCG-Zn NMs.

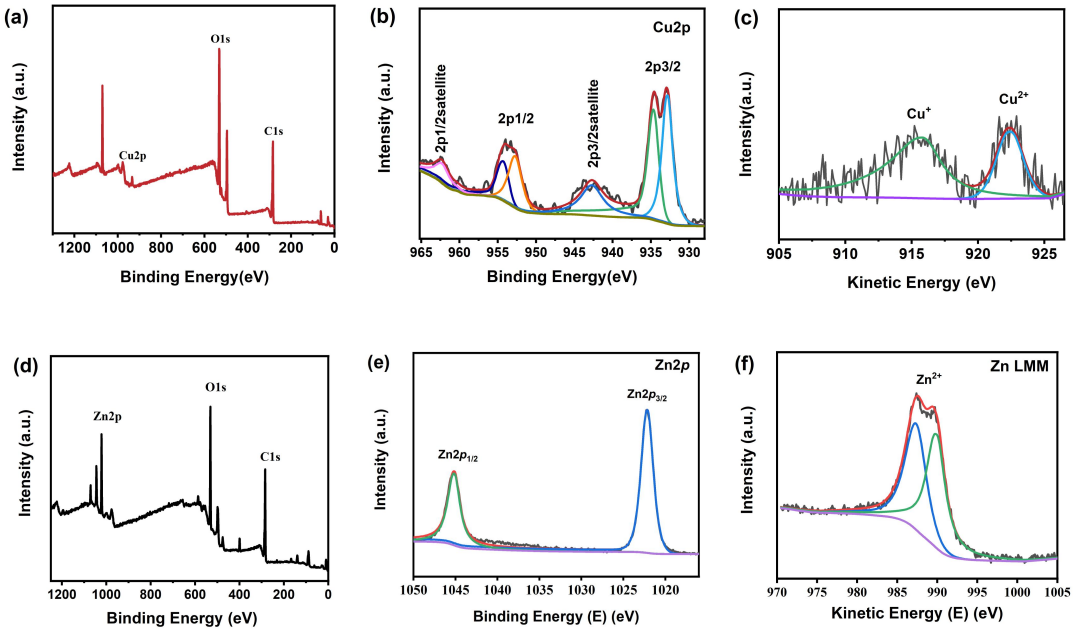


**Figure 3.** (a) XPS spectra of EGCG-Cu NMs, (b) Cu 2*p* and (c) Cu LMM Auger spectra of EGCG-Cu NMs; (d) XPS spectra of EGCG-Zn NMs, (e) Zn 2*p* and (f) Zn LMM Auger spectra of EGCG-Zn NMs.

As shown in Figure 3, the XPS spectrum of Cu 2*p* exhibited prominent peaks at 934 eV for Cu 2*p*3/2 and 955 eV for Cu 2*p*1/2. The Cu LMM spectrum showed different kinetic energy states of $Cu^{+}$ and $Cu^{2+}$ ions in EGCG-Cu NMs. Similarly, the XPS spectrum of Zn 2*p* showed

prominent peaks at 1022 eV for Zn 2*p*3/2 and 1045 eV for Zn 2*p*1/2. The Zn LMM showed the $Zn^{2+}$ state in the EGCG-Zn NMs.

3.3 Evaluation of NMs properties

The antioxidant activity of EGCG NMs was evaluated by DPPH, hydroxyl radical (·OH) and $H_2O_2$ scavenging assays. As shown in Figure 4, the DPPH, ·OH and $H_2O_2$ scavenging efficiencies of EGCG NMs were individually increased with higher concentrations. The DPPH scavenging efficiency could reach 80% at the concentration of 0.5 mg/mL of EGCG NMs. Furthermore, the ·OH scavenging result indicated that 60% of ·OH could be reduced by EGCG NMs at a concentration of 0.5 mg/mL, and the ·OH scavenging efficiency could reach 90% when the concentration of NMs was over 4 mg/mL. The $H_2O_2$ scavenging efficiency of EGCG NMs, as shown in Figure 4b, was found to be significantly increased from about 30% to 98% in proportion to the concentration of 1~4 mg/mL, compared to the untreated control group of $H_2O_2$.

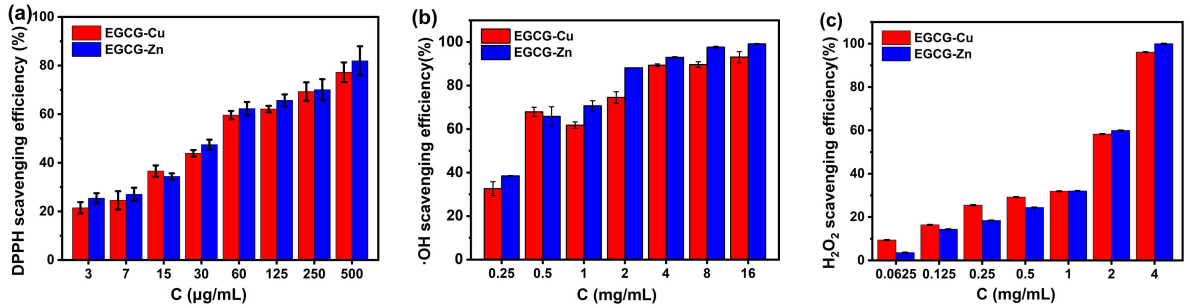


**Figure 4.** (a) DPPH, (b) ·OH and (c) $H_2O_2$ scavenging efficiency of EGCG NMs at different concentrations.

To evaluate the antibacterial activity of NMs, the MBC assay against *C. acnes* and *M. furfur* was performed on EGCG-Cu NMs. As shown in Figure 5, the MBC concentration of EGCG, $Cu^{2+}$ and EGCG-Cu NMs were tested separately at different concentrations. The MBC of EGCG-Cu NMs was found to be approximately 1 mg/mL for *M. furfur*, whereas the MBC of $Cu^{2+}$ or EGCG was found to be greater than 2 mg/mL for *M. furfur*. Furthermore, the MBC of NMs was found to be 0.93 mg/mL for *C. acnes*, suggesting an increased potential for anti-acne properties.

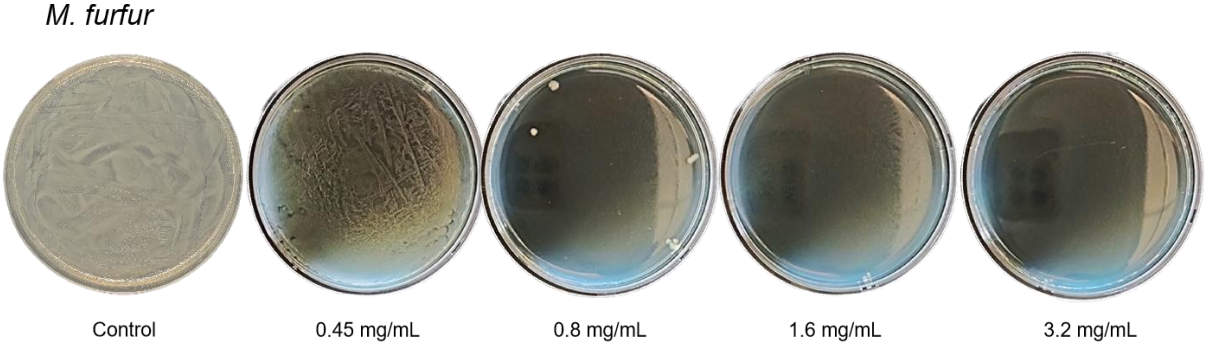

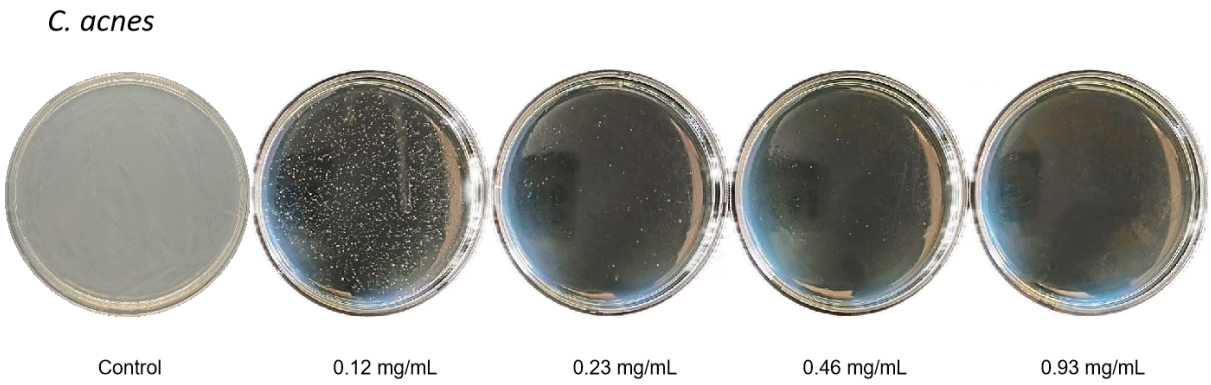


**Figure 5.** MBC assay of EGCG-Cu NMs *against Malassezia furfur* and *Cutibacterium acnes.*

## 4. Discussion

In this work, we have developed a simple, green and sustainable process for the synthesis of multifunctional NMs by coordination of EGCG and metal ions. The microstructure and properties of the NMs were then characterized using UV-vis, FTIR and XPS spectroscopy. The UV-vis spectra showed a coincident absorption wavelength shift from 274 nm to 300-350 nm between EGCG and EGCG NMs, indicating that phenolic ligand-metal charge transfer (LMCT) may occur between EGCG and $Cu^{2+}$ or $Zn^{2+}$. The successful formation of EGCG NMs composites with different absorption characteristics compared to EGCG was also demonstrated.

In addition, the FTIR spectra showed variation of the characteristic absorption peaks of EGCG and EGCG-Cu NMs, indicating different microstructures between EGCG and its NMs. The FTIR absorption spectra of EGCG showed that the characteristic absorption peak centered at 3357 $cm^{-1}$ was shifted to 3431 $cm^{-1}$ and 3416 $cm^{-1}$ due to the altered hydrogen bonding of phenolic hydroxyl groups in EGCG-Cu and EGCG-Zn NMs, respectively. The disappearance of the absorption peak at 1692 $cm^{-1}$ in the spectrum of EGCG suggested that the metal ion may have formed a coordination bond with the carbonyl oxygen, resulting in a weakening of the C=O double bond property or a conversion to a single bond (e.g. formation of a metal-oxygen coordination bond), resulting in the disappearance of the characteristic peak.

The characteristic absorption peaks centred at 1086 $cm^{-1}$ and 627 $cm^{-1}$ were apparently shifted between EGCG and EGCG NMs. It was suggested that metal coordination could alter the intramolecular hydrogen bonding network, which further affected the frequency of the C-O stretching vibration of the phenolic hydroxyl group at 1086 $cm^{-1}$ and the out-of-plane bending vibration of the C-H in the benzene ring at 627 $cm^{-1}$.

Understanding the oxidation state and chemical environment of metal ions in NMs is crucial for applications such as catalysis, biological function and drug delivery. The XPS analysis of EGCG NMs provided significant insight into the electronic states of Cu within these structures. The XPS spectrum of Cu 2*p* showed prominent peaks at 934.7 eV and 932.5 eV for Cu 2*p*3/2 and 954.4 eV and 952.8 eV for Cu 2*p*1/2. The strong satellite peaks at 942.7 eV for Cu 2*p*3/2 and 962.5 eV for Cu 2*p*1/2 were observed. These peaks indicated the presence of Cu in different oxidation states within the NMs, suggesting a complex chemical environment. This finding

implied that copper existed in the multiple states within the EGCG NMs, which may significantly influence the redox properties and reactivity of the NMs. Correspondingly, the LMM spectrum showed different kinetic energy states of $Cu^{+}$ and $Cu^{2+}$ ions, indicating the different oxidation states and the local chemical environment of the Cu ion within the NMs. This variation in kinetic energy may provide further insight into the dynamic behavior and potential applications of these copper states in EGCG NMs.

In a similar manner, the XPS spectrum of Zn 2*p* showed prominent peaks at 1022.2 eV for Zn 2*p*3/2 and 1045.2 eV for Zn 2*p*1/2, suggesting that Zn was predominantly present as $Zn^{2+}$ in the NMs. It could be inferred that the variation of the LMM parameter of EGCG-Zn NMs (2011.8 eV) was the consequence of the coordination interaction between Zn and EGCG in the NMs.

The intrinsic peroxidase-like and catalase-like antioxidant activities of NMs have attracted much attention. Consequently, *in vitro* DPPH, ·OH, and $H_2O_2$ radical scavenging assays were then performed to evaluate the antioxidant activity of EGCG NMs. The results demonstrated that the polyphenols present in the NMs exhibited multiple antioxidant effects at low concentrations. Compared to the metal ion and EGCG, the scavenging efficiencies of ·OH and $H_2O_2$ of EGCG-Zn were significantly enhanced and a positive correlation between these enhancements and the concentration was observed (data not shown).

The enhancement of $H_2O_2$ catalysis, which has the capacity to generate free radicals, also provides an opportunity to eliminate biofilm [16], a special bacterial community that helps bacteria to develop drug resistance by limiting the penetration of antibiotics or other biocides into the protective, organic matrix [17]. As demonstrated in earlier studies, $Cu^{2+}$ coupling NMs have shown robust antibacterial effects at extremely low doses against both Gram-positive and Gram-negative bacteria in vitro. It is evident that the high redox potential of copper ($Cu^{+}$) renders it highly efficient in catalyzing the trace $H_2O_2$ in the extracellular environment of bacterial cells to generate ROS. The assembled Cu NMs demonstrated remarkable efficacy against pathogenic bacterial infections and contributes significantly to collagen deposition and skin regeneration [18]. Since *C. acnes* and *M. furfur* are the predominant microbes on the skin, the antimicrobial activity of Cu NMs was evaluated using MBC assays. We found a unique synergistic antimicrobial activity exhibited by Cu NMs, in comparison to polyphenol or $Cu^{2+}$, individually. The results showed that the MBC of EGCG-Cu NMs was approximately 1.0 mg/mL for *M. furfur*, whereas $Cu^{2+}$ and EGCG were required at much higher concentrations for *M. furfur*, indicating enhanced synergistic antimicrobial efficacy in the composite of EGCG-Cu NMs. In addition, the MBC of EGCG-Cu NMs was determined to be 0.93 mg/mL for *C. acnes*, suggesting the potential for further investigation into the activity of Cu NMs in the treatment of acne or other skin microbial imbalance.

Considering the challenges associated with the control process of synthesis and dispersion of substances within skin care formulations, the application of versatile NMs offers a promising solution. It has been demonstrated that these NMs exhibit enhanced stability when dispersed in water, thereby facilitating their use in a wider range of applications, including oil control, anti-dandruff shampoo, oil control and anti-dandruff scalp serum. In conclusion, NMs have been demonstrated to possess excellent stability, multiple antioxidant and antibacterial properties, which have promising application potential in scalp and skin care.

## 5. Conclusion

In this study, a novel multifunctional nanozyme technology was proposed, and a series of versatile NMs were developed in a green and sustainable manner, without using organic solvents or complicated processes. A variety of analytical techniques were employed to investigate the microstructure and efficacy of these NMs. It was established that EGCG NMs demonstrated a high degree of versatility in terms of their antioxidant activity, and that NMs exhibited a synergistic effect in terms of their antimicrobial properties when compared with polyphenols or metal ions. Furthermore, the novel and versatile NMs have successfully been developed into a variety of skin care products, which can be further customized or tailored designed. These products have the potential to serve as a multifunctional strategy for skin treatment, particularly in cases of oxidant-stressed skin problems.

## References

[1] H. Wang, K. Wan, X. Shi, Adv Mater, 31 (2019) e1805368.
[2] J. Wu, X. Wang, Q. Wang, Z. Lou, S. Li, Y. Zhu, L. Qin, H. Wei, Chem Soc Rev, 48 (2019) 1004-1076.
[3] H. Ejima, J.J. Richardson, K. Liang, J.P. Best, M.P. van Koeverden, G.K. Such, J. Cui, F. Caruso, Science, 341 (2013) 154-157.
[4] Y. Yu, G. Chen, J. Guo, Y. Liu, J. Ren, T. Kong, Y. Zhao, Materials Horizons, 5 (2018) 1137-1142.
[5] H. Geng, Q.-Z. Zhong, J. Li, Z. Lin, J. Cui, F. Caruso, J. Hao, Chemical Reviews, 122 (2022) 11432-11473.
[6] F. Gao, W. Liang, Q. Chen, B. Chen, Y. Liu, Z. Liu, X. Xu, R. Zhu, L. Cheng, Nanomaterials, 14 (2024) 389.
[7] H. Byun, G.N. Jang, M.-H. Hong, J. Yeo, H. Shin, W.J. Kim, H. Shin, Nano Convergence, 9 (2022) 47.
[8] D. Jiang, D. Ni, Z.T. Rosenkrans, P. Huang, X. Yan, W. Cai, Chem Soc Rev, 48 (2019) 3683-3704.
[9] L. Qin, Y. Hu, H. Wei, Nanozymes: Preparation and Characterization, in: X. Yan (Ed.) Nanozymology: Connecting Biology and Nanotechnology, Springer Singapore, Singapore, 2020, pp. 79-101.
[10] E.Z. Gomaa, Journal of Cluster Science, 33 (2022) 1275-1297.
[11] F. Silva, F. Veiga, C. Cardoso, F. Dias, F. Cerqueira, R. Medeiros, A. Cláudia Paiva-Santos, Microchemical Journal, 202 (2024) 110801.
[12] Y. Tang, Y. Han, J. Zhao, Y. Lv, C. Fan, L. Zheng, Z. Zhang, Z. Liu, C. Li, Y. Lin, Nano-Micro Letters, 15 (2023) 112.
[13] R. Apak, A. Calokerinos, S. Gorinstein, M.A. Segundo, D.B. Hibbert, İ. Gülçin, S.D. Çekiç, K. Güçlü, M. Özyürek, S.E. Çelik, L.M. Magalhães, P. Arancibia-Avila, Pure and Applied Chemistry, 94 (2022) 87-144.
[14] J. Rumpf, R. Burger, M. Schulze, Int J Biol Macromol, 233 (2023) 123470.

[15] S. Caillet, H. Yu, S. Lessard, G. Lamoureux, D. Ajdukovic, M. Lacroix, Food Chemistry, 100 (2007) 542-552.
[16] L. Gao, K.M. Giglio, J.L. Nelson, H. Sondermann, A.J. Travis, Nanoscale, 6 (2014) 2588.
[17] L. Gao, Y. Liu, D. Kim, Y. Li, G. Hwang, P.C. Naha, D.P. Cormode, H. Koo, Biomaterials, 101 (2016) 272-284.
[18] T. Liu, M. Ma, A. Ali, Q. Liu, R. Bai, K. Zhang, Y. Guan, Y. Wang, J. Liu, H. Zhou, Nano Today, 54 (2024) 102071.